Advances in Materials Science and Engineering

WILEY

RESEARCH ARTICLE OPEN ACCESS

Enhancement of Polyethylene Terephthalate Rheological Properties via Chain Extension and Branching: A Design of Experiment Approach

Ilaria Cusano[1] | Laura Campagnolo[2] | Salvatore Costanzo[1] | Marco Aurilia[2] | Nino Grizzuti[1]

[1]Department of Chemical, Materials and Production Engineering, University of Naples Federico II, P.le Tecchio 80, Naples 80125, Italy | [2]Gurit, Volpiano 10088, Italy

Correspondence: Ilaria Cusano (ilaria.cusano@unina.it)

Received: 8 July 2025 | **Revised:** 19 December 2025 | **Accepted:** 26 December 2025

Academic Editor: Mohammad Rezwan Habib

Keywords: branching | chain extension | polyethylene terephthalate | reactive extrusion | rheology

ABSTRACT

Upgrading recycled polyethylene terephthalate (PET) for high-value applications requires enhanced viscoelastic properties that are difficult to achieve with single chain extenders. This study investigates the synergistic effect of pyromellitic dianhydride (PMDA, tetrafunctional) and 1,3-phenylene-bis-2-oxazoline (PBO, bifunctional) on virgin and recycled PET using the Design of Experiment methodology. Real-time rheological monitoring, combined with a heuristic kinetic analysis, enabled the identification of the reaction mechanisms and their evolution over time. Subsequently, the linear viscoelasticity analysis of the reacted samples revealed that the dual-additive system led to an increase of two orders of magnitude in zero-shear viscosity (compared to one order for PMDA alone) and three orders of magnitude in relaxation times, reaching approximately 20 s. Critical differences between virgin and recycled PET responses are identified, with recycled material showing enhanced properties at high additive concentrations due to higher carboxyl end-group content. These findings provide a systematic approach for upgrading postconsumer PET to meet industrial performance requirements for foaming and blow molding applications.

1 | Introduction

Polyethylene terephthalate (PET) is a linear polymer composed of terephthalic acid (TPA) and ethylene glycol (EG) repeating units [1]. It is widely used in the manufacturing of bottles and other forms of packaging. Therefore, its production makes a significant contribution to global plastic consumption. For example, European manufacturing of virgin PET (vPET) reached 2.3 million tonnes in 2022 [2].

Due to its massive use in disposable items, PET is one of the most concerning pollutants worldwide [3–5]. Consequently, its recycling is currently a key objective within the framework of a circular economy strategy [6]. Among the available technologies, mechanical and chemical recycling are most commonly employed [7, 8]. Chemical recycling involves total or partial depolymerization of PET chains through the use of water, methanol, or EG itself [9]. Despite being an effective technique, it is less frequently applied because of its high cost. Mechanical recycling is a less complex process that is based on the collection, sorting, and melting of PET waste with the objective of reprocessing it [10].

During mechanical recycling, PET chains undergo multiple scissions as a result of high temperatures [11], the presence of contaminants [12], and traces of moisture [13]. This manifests as a reduction in the molecular weight of the polymer and a general worsening of its viscoelastic and mechanical properties in both the melt and the solid phase [6, 14]. Various technologies are available for the repurposing of recycled.

Various technologies are available for the repurposing of recycled PET (rPET), including injection molding [15], chemical reconversion [16], and composite reinforcement for additive manufacturing [17–20]. The method under consideration in this work is reactive extrusion [21], which allows the reuse of post-consumer PET for the production of lightweight materials when combined with polymer foaming. Reactive extrusion is based on the chain extension mechanism, which involves reacting linear PET chains with selected additives, resulting in a branched polymer architecture. Branching improves the viscoelastic properties of the material, optimizing it for advanced processing applications such as foaming and blow molding. The additives, known as chain extenders, can have different chemistries [22] (epoxides, oxazolines, or isocyanates) and different functionalities. Depending on the latter, the chain extension reaction can generate macromolecules with different molecular architectures, such as stars with varying numbers of arms and, in some cases, even dendritic structures [6]. The combination of different chain extender types may result in varying effects on viscoelastic properties. This topic has been addressed by numerous authors in the literature. The effect of pyromellitic dianhydride (PMDA), a tetrafunctional additive, on the thermal and viscoelastic behavior of recycled PET was investigated by Incarnato et al. [23]. They found that rPET, modified with optimal quantities of PMDA under appropriate conditions, recovers the essential features for blow molding. Similarly, Liu et al. [24] demonstrated that long-chain branching resulting from the reaction between PET and PMDA improved the rheological properties of the polymer melt. The same system has also been characterized by Härth and Dörnhöfer [25], along with PET modified with Joncryl, a multifunctional epoxy. This work illustrates how the combination of the two additives, when added to PET in two distinct stages, optimizes the polymer for film blowing by providing the essential extensional properties. Arayesh et al. [26], on the other hand, investigated the impact of four distinct chain extenders and the diverse molecular structures they form with linear PET on rheological and thermal properties. Several other researchers have made similar efforts to modify vPET and rPET using the chain extension mechanism [27–32].

It is clear from the above-mentioned literature that PET reactive extrusion enables the development of tailored, optimized materials that meet the specific requirements of the industrial production processes. However, most studies have focused on single-chain extenders, leaving the potential synergistic effects of combining additives with complementary functionalities largely unexplored. The present study investigates the combined use of PMDA and 1,3-phenylene-bis-2-oxazoline (PBO) as chain extenders for both virgin and recycled PET. This combination was selected based on the complementary reactivity of the two additives: PMDA is a tetrafunctional molecule that reacts with the terminal hydroxyl groups of the linear PET chains via its anhydride groups [33], whereas PBO is a bifunctional molecule that links to the carboxyl terminal groups of the linear PET chain [34] (see Figure 1 [26, 35]). This dual reactivity enables the formation of complex molecular architectures, combining chain extension and branching, that cannot be achieved with either additive alone. Therefore, adjusting the relative amounts of PMDA and PBO in the reactive mixture allows fine-tuning of the viscoelastic properties through the presence of the different molecular structures of the species formed during the reactive extrusion process. A systematic Design of Experiment (DoE) approach was employed to evaluate various additive combinations through a comprehensive rheological characterization including dynamic time sweep tests (DTST) for reaction kinetics and dynamic frequency sweep tests (DFST) for viscoelastic behavior assessment. The results demonstrate that the dual-additive system produces substantial improvements in zero-shear viscosity and relaxation time. These findings indicate that the PMDA-PBO combination enables effective property tuning for advanced processing applications while offering promising strategies for upgrading recycled materials.

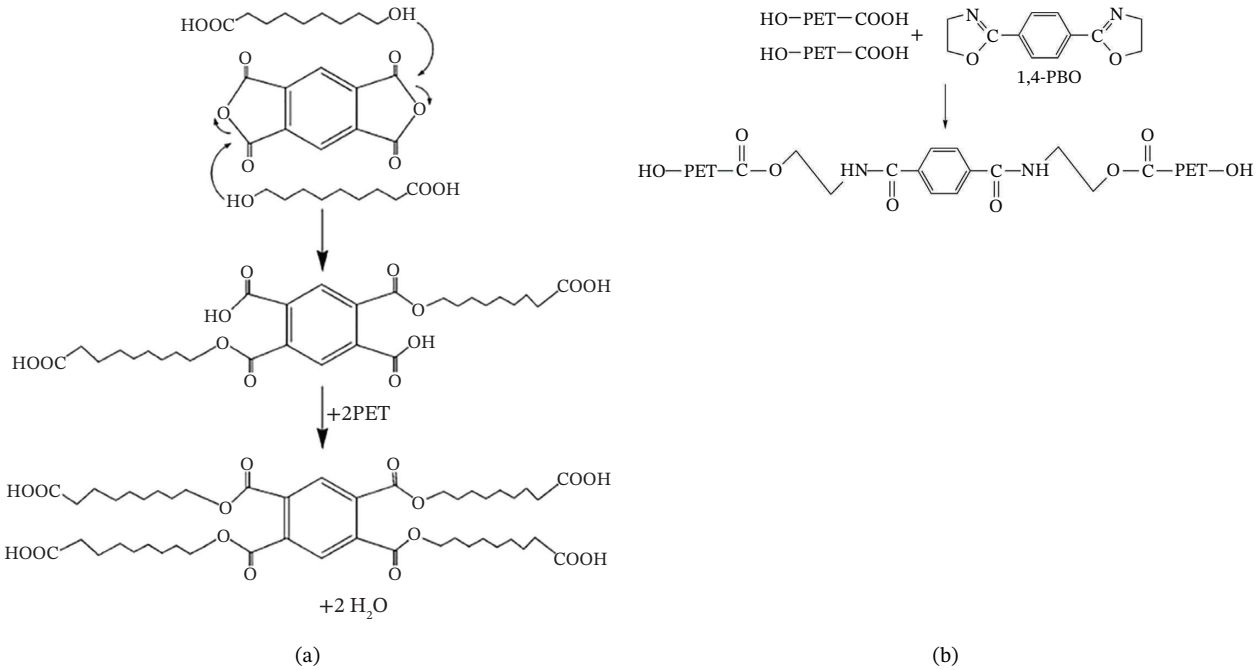

FIGURE 1 | Reactions of (a) PMDA and (b) PBO with PET. Reprinted from references [26, 35].

TABLE 1 | Factors and levels.

	Level 1	Level 2	Level 3
Factor 1			
PET grade	vPET	rPET	—
Factor 2			
PMDA content (%)	0	0.15	0.3
Factor 3			
PBO content (%)	0	0.2	0.4

Beyond the specific formulations investigated, the novelty of this work lies in the adoption of a DoE–driven framework that enables a rational, a priori design of PET molecular architectures. By explicitly linking additive concentration, reaction kinetics, and rheological response, this approach moves beyond empirical optimization and provides a transferable methodology for tailoring PET properties through reactive extrusion.

2 | Experimental

2.1 | DoE

The DoE was based on the Six Sigma methodology [36]. First, the factors, i.e. the variables, and the levels, i.e., the values of each variable, were defined. Factors and levels are listed in Table 1.

The concentration levels for PMDA and PBO were selected based on industrial feasibility considerations, balancing performance enhancement with cost-effectiveness. The selected ranges (0.15%–0.30% for PMDA and 0.2%–0.4% for PBO) represent typical industrial concentrations for PET chain extension, where significant property improvements can be achieved while maintaining economic viability for large-scale recycling applications. Since Factor 1 has one less level compared to Factors 2 and 3, a *mixed-level factorial design* was applied: every level of each factor was combined with all levels of the other factors. The sequence of mixtures to be tested was then built, which combined PET grades and chain extenders. This was achieved by using Minitab software (Minitab LLC, USA), which provided the list of tests to be performed on samples in random order, considering one replica per batch. The sequence is shown in Table 2.

For each mixture, a single batch was produced and then analyzed.

2.2 | Materials

Granules of the raw materials, namely the two PET grades and the chain extenders, were kindly provided by the Valplastic company (Valplastic S.r.l., Italy). The virgin grade PET has a glass transition temperature of 82°C and a melting temperature of 243°C. For the recycled material, the glass transition temperature is equal to 85°C and the melting temperature is 250°C. The chain extenders were supplied as masterbatches at known concentrations of PMDA and PBO. PMDA is a tetrafunctional chain extender with an anhydride functional group, which can lead to the formation of macromolecules with a four-arm star structure. PBO, conversely, is a bifunctional, oxazoline-based molecule that allows the creation of elongated linear chains.

2.3 | Sample Preparation

The granular mixtures were prepared by weighing appropriate amounts of the components. Each mixture was then ground using a cryo-miller, ensuring that the resulting powders were fine enough to guarantee the optimal mixing of the components. This was confirmed through the repetition of rheological tests on several samples. An example is provided in the supporting information. Finally, the samples were stored in a dynamic vacuum oven at 70°C for at least 12 h to remove all moisture residues of the powders.

TABLE 2 | List of samples.

Standard order	Run order	PET grade	PMDA content	PBO content
6	1	rPET	0.15	0.4
10	2	vPET	0	0
11	3	vPET	0	0.2
9	4	rPET	0.3	0.4
7	5	rPET	0.3	0
15	6	vPET	0.15	0.4
12	7	vPET	0	0.4
13	8	vPET	0.15	0
16	9	vPET	0.3	0
18	10	vPET	0.3	0.4
14	11	vPET	0.15	0.2
3	12	rPET	0	0.4
5	13	rPET	0.15	0.2
2	14	rPET	0	0.2
1	15	rPET	0	0
4	16	rPET	0.15	0
8	17	rPET	0.3	0.2
17	18	vPET	0.3	0.2

2.4 | Rheology Tests

Rheological tests were performed with an ARES-G2 rotational rheometer (TA Instruments, USA) equipped with an air-fed convection oven for temperature control. Parallel plates with a 25 mm diameter were selected as the measuring geometry. The mixtures were loaded onto the bottom plate using a metallic ring to avoid dust dispersion caused by the air flow inside the oven. After melting of the powders, the ring was removed and the upper plate was lowered to a gap of approximately 1 mm.

A specific test procedure was designed to investigate the branching reaction and the relaxation phenomena of the polymer melt. To observe the evolution of the reaction with time, DTSTs were carried out for 1200 s at $T = 260°C$, with strain amplitude and angular frequency set at 5% and 1 rad/s, respectively. At the end of each DTST test, a DFST was performed in the angular frequency range of (100, 0.5) rad/s, using the same temperature and strain amplitude as in the previous test. As PET is extremely sensitive to high temperatures and oxygen in the air stream, this relatively narrow range of angular frequencies was chosen to prevent degradation phenomena that might compromise the accuracy of the rheological measurement. However, in such a narrow frequency range, it was not possible to obtain the terminal flow behavior. For this reason, the terminal regime was extrapolated according to an empirical procedure described in Section 2.6.

2.5 | Data Processing: Reaction Kinetics

It was observed that, due to the high-temperature powder loading procedure, the acquisition of the transient complex viscosity was delayed, leading to the loss of the initial short-time region, which is crucial for kinetic analysis. To overcome this limitation and reconstruct the complete transient profile, a fitting procedure was applied to estimate the delay time and to appropriately shift the viscosity curves. In order to model the reactive extrusion process, an estimation of the characteristic reaction time is also required. To this end, the reaction between PET and the two chain extenders was assumed to follow first-order kinetics. Although this assumption represents a simplification of the actual reactive system, it provides a fitting expression that describes the experimental evolution of the complex viscosity with reasonable accuracy. Moreover, the inverse of the kinetic constant obtained from the fit allows a direct estimation of the characteristic reaction time. Therefore, based on the considerations outlined above, the evolution of the complex viscosity was treated as analogous to the conversion degree of a first-order reaction, as expressed by equation (1) [37].

$$\frac{\eta^*(t) - \eta_0}{\eta_\infty - \eta_0} = x(t), \tag{1}$$

where η_0 and η_∞ refer to the viscosity of the pristine vPET and the steady-state viscosity attained during DTSTs, respectively.

Based on the assumption of first-order kinetics, the delay time due to high-temperature loading procedures t_s and the kinetic constant k can be obtained by using equation (2):

$$\eta^*(t) = \eta_0 + (\eta_\infty - \eta_0)\left(1 - e^{-k(t-t_s)}\right). \tag{2}$$

Note that η_∞ is experimentally obtained from the long-time plateau of η^*. Likewise, η_0 can be measured independently from measurements carried out without the chain extenders. For this reason they are not considered as adjustable parameters.

2.6 | Data Processing: Linear Viscoelasticity

As stated in Section 2.4, because of fast degradation at high temperature, the linear viscoelastic moduli of the samples were measured in a narrow frequency range where the terminal flow behavior could not be observed. Therefore, to provide at least an empirical estimate of the zero shear viscosity of the materials, we extrapolated the terminal regime based on a Maxwell fit of the experimental data. To this end, the viscoelastic moduli of each sample were fitted with a 7-mode Generalized Maxwell Model using the Reptate [38] software. Then, the fitting parameters, namely the moduli and relaxation times of the different modes, were imported into a custom MATLAB routine which extrapolated the viscoelastic moduli from 0.5 to 0.01 rad/s. It should be noted that such an extrapolation is not generally valid and might lead to significant errors in the estimation of the moduli outside the measured frequency range. However, a series of validation tests were conducted to evaluate the efficacy of the procedure that had been developed specifically for this case. Some examples of the validation procedure are reported in the Supporting Information (available here).

Based on the frequency response, van Gurp–Palmen (vGP) plots were constructed, which reproduce the phase angle, δ, as a function of the complex modulus, G^*. These quantities were derived from:

$$\tan\delta = \frac{G''}{G'}, \tag{3}$$

$$G^* = \left(G'^2 + G''^2\right). \tag{4}$$

Finally, the complex viscosity was derived from the viscoelastic moduli, using (equation (5)):

$$\eta^* = \frac{G^*}{\omega}. \tag{5}$$

For each sample, the zero-frequency viscosity was extracted from the plateau of the complex viscosity in the low-frequency range. The relaxation time was obtained as the inverse of the frequency corresponding to the intercept of the viscosity plateau with the straight line fitting the high-frequency shear-thinning regime.

2.7 | Data Analysis: Linear Viscoelasticity

Zero-frequency viscosities and relaxation times data were imported into the Minitab software, which generated the variability charts, the Pareto charts, and the interaction plots. This allowed for assessment of the efficacy of the overall experimental campaign.

3 | Results and Discussion

3.1 | Chain Extension/Branching Reaction

Figure 2 shows the evolution of the chain extension/branching reaction over time for the two sets of samples, namely vPET-based and rPET-based samples. The various effects of the two

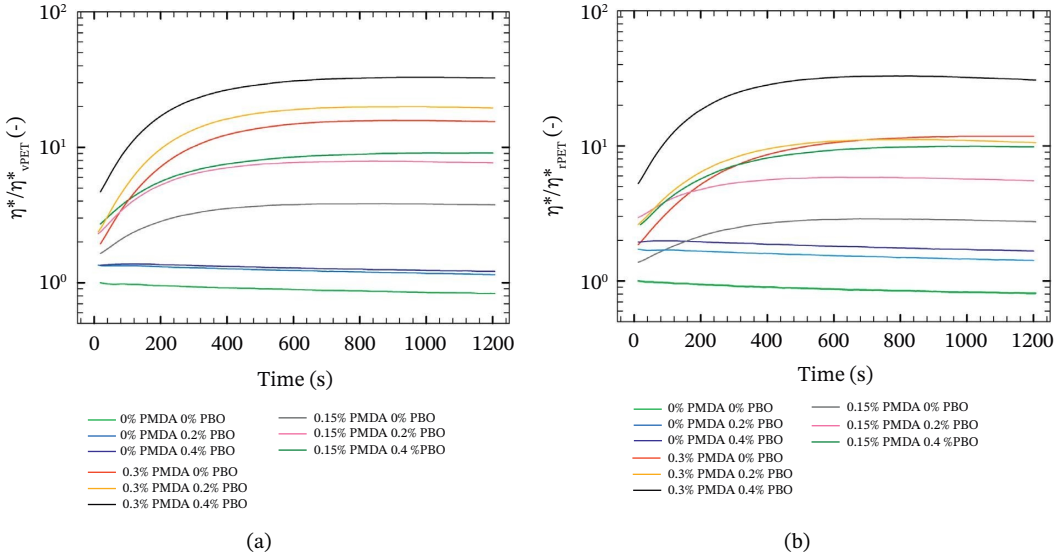

FIGURE 2 | Chain extension/branching reaction of PET: complex viscosities (η^*) of polymer melts vs. time for (a) virgin PET samples: curves compare formulations with 0%–0.3% PMDA and 0%–0.4% PBO. (b) Recycled PET samples: curves show the same range of PMDA and PBO concentrations. All curves were normalized by the corresponding neat PET viscosity value. The complex viscosity loss is approximately 17% for vPET-based samples and 19% for rPET-based samples due to thermo-oxidative degradation.

chain extenders are evident for both PET grades. Mixtures containing only PBO exhibit an increase in complex viscosity compared to neat PET, resulting from PET linear chain extension. PBO extends PET chains by linking two terminal carboxylic acid groups, leading to the formation of a polyamide–polyester copolymer [39].

The increase in the average molecular weight of the macromolecules causes the viscosity to increase [40]. No intermediate transient behavior is observed, probably because this chain extension reaction occurs so rapidly that it cannot be detected by rheological measurements, given that it lasts approximately 3 min [35] and the first measurement is only taken around 200 s after sample loading.

A different response can be observed for PMDA-modified samples. Here, the complex viscosity undergoes a rapid increase in the initial stage, indicating that the branching reaction is proceeding. This involves the formation of ester bonds between the PET hydroxyl end groups and the PMDA anhydride group [41]. Since PMDA is a tetrafunctional molecule, it can first lead to chain elongation and then to the formation of star-shaped branched structures with up to four arms. [42]. All η^* curves reach a steady state, which suggests the end of the reaction.

Samples modified with both PMDA and PBO show a transient behavior that combines the above-mentioned features. In both PET grades, a slight decrease in complex viscosity is observed over long times, which can be attributed to the thermo-oxidative degradation of the polymer melts [43].

The achieved viscosity values of the vPET-based samples are overall higher compared to those of rPET-based ones. This can be attributed to the fact that the material has not undergone previous processes such as recycling, which can lead to mechanical chain degradation [44]. In the case of recycled samples, the average molecular weight of the polymer melt is reduced, causing a corresponding drop in viscosity, which is evident in Figure 2(b) for the rPET-based samples. A further significant distinction between the two PET grades is that, in the case of vPET-based samples, an increase in the additive content corresponds to an increase in the viscosity value. This relationship is not observed for rPET-based samples, which exhibit a disordered overall response. This discrepancy may be attributed to the difference in carboxyl end groups between the two PET grades. Indeed, during the recycling process, the formation of COOH terminal groups in the polymer is uncontrolled [13], which results in subsequent processing of rPET being uneven compared to vPET. This can also be observed from the reaction rate coefficients evaluated by fitting the curves presented in Figure 2 with equation (2). The average reaction rate coefficients were found to be as follows: for vPET they are $4.6{\cdot}10-3\,s^{-1}$ and $3.2{\cdot}10-3\,s^{-1}$ for 0.15% PMDA and 0.30% PMDA, respectively, while for rPET they are $5.2{\cdot}10-3\,s^{-1}$ in the case of 0.15% PMDA and $3.9{\cdot}10-3\,s^{-1}$ in the case of 0.30% PMDA. It appears that the PBO concentration does not exert any significant influence on the rate of chain extension/branching reactions, unlike PMDA. Moreover, the reaction seems to proceed faster when the dianhydride concentration is lower. One possible explanation could be that, in the initial chain extension phase, PMDA is more reactive with PET than in the second branching phase, where two carboxyl end groups have already formed in the macromolecule [45].

A reduction in the quantity of PMDA in the sample will result in a faster reaction with the linear PET chains, leading to the formation of extended structures, and an earlier termination of the reaction.

3.2 | Linear Viscoelasticity of Reacted Samples

In order to evaluate the effect of the two additives on the rheological properties of the final samples, we analyzed them once the reaction was complete. The chain extension/branching dynamics of the polymer melts can be observed in Figure 3, which

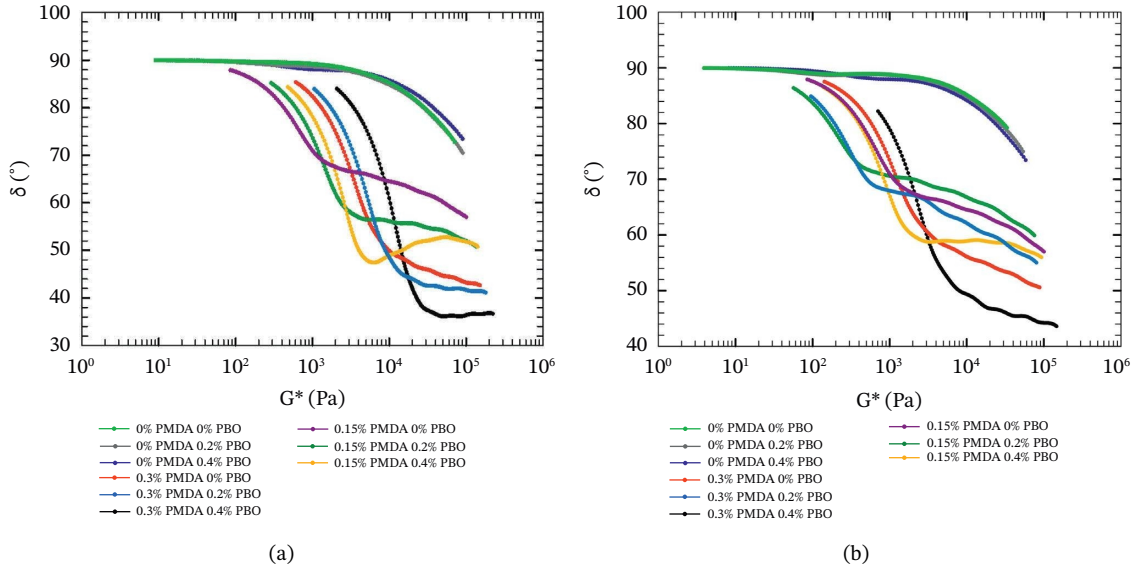

FIGURE 3 | Van Gurp–Palmen plots of PET melts after the chain extension reaction. Data were obtained following the procedure outlined in Section 2.6. Phase angle (δ) is shown as a function of the complex modulus ($|G^*|$) for different concentrations of PMDA and PBO. (a) Virgin PET samples: curves compare formulations with 0%–0.3% PMDA and 0%–0.4% PBO. (b) Recycled PET samples: curves show the same range of PMDA and PBO concentrations.

shows the vGP plots, obtained by following the procedure described in Section 2.6.

The vGP plot shows the phase angle, δ, as a function of the complex modulus, G^*. The shape of the curve gives insight into the branching phenomena that occur within a polymer system [46]. In this context, such a graph is a key tool, as it assesses the impact of additives and their concentration [6]. In the case of linear chain polymers, the curve has a single inflection point, and no particular deviations or peaks are evident. When branching begins, the curves show a shoulder, which becomes more pronounced as the degree of branching of the polymer increases, until a local minimum point possibly appears [47]. As illustrated in Figure 3(a)), the vPET samples modified with PBO only behave, as expected, as linear chain polymers, with no hint of bumps. When PMDA is added instead, the shoulder appears in the curves and becomes more significant as the chains lengthen and the degree of branching increases. The occurrence of these two phenomena is contingent on the increasing concentrations of PBO and PMDA, as evidenced by the progressive deviation of the trends (from the purple curve to the black curve) from linear behavior (green, grey, and blue curves). The greatest departure from linearity is observed in the samples with the highest concentration of additives, pointing to a stronger ramification. This also holds true for the rPET-based samples, although, as already seen in Section 3.1 (Figure 2(b)), the arrangement of the curves is less systematic.

In addition to the vGP plots, as part of the DoE, the complex viscosity curves of the reacted samples were also evaluated. The resulting data are presented in Figure 4. Figure 4(a)) shows the complex viscosity profiles as a function of angular frequency for all vPET-based samples. The general features are consistent with those observed previously. Compared to neat vPET, the PBO-modified samples exhibit complex viscosities with analogous morphology but increasing magnitudes. In both cases the overall trend is Newtonian, with a small hint of thinning at the highest frequencies. This is typical of relatively short, linear chain polymers, which exhibit terminal relaxation behavior over nearly the entire frequency range investigated. The situation is different for samples that have also been modified with PMDA. Thinning appears earlier and is more pronounced as the concentration of the branching agent increases. This phenomenon can be explained by an increase in the polymer melt polydispersity index and molecular weight [48]. The alignment of larger entangled macromolecules with different architectures results in more pronounced shear thinning behavior [49]. Nevertheless, an increase in the zero-frequency viscosity, i.e., the complex viscosity value in the lowest frequency range, is consistently observed in all samples. The same is also true for rPET-based samples, although the results exhibit less consistency.

Figure 5 summarizes the dependence of the zero-shear viscosity upon polymer source and chain extender composition. It demonstrates the overall increase in the molecular weight of the macromolecules as a consequence of chain extension and branching phenomena.

3.3 | Data Analysis

As the final phase of the DoE, data were processed to allow for the assessment of the efficacy of the experimental campaign. Figures 6 and 7 show the variability chart of zero frequency viscosity and relaxation time of the polymer melts, after the chain extension/branching reaction was complete. These graphs collect all the viscoelastic responses, thus facilitating the evaluation of the influence of each factor (and their combination) on the aforementioned variables.

The zero-frequency viscosity variability chart (Figure 6) confirms what has been said above. In all cases, the increase in additive concentration leads to an increase in the molecular weight of the two PET grades because of chain elongation and branching phenomena. Systematically higher viscosity values are recorded for vPET-based samples.

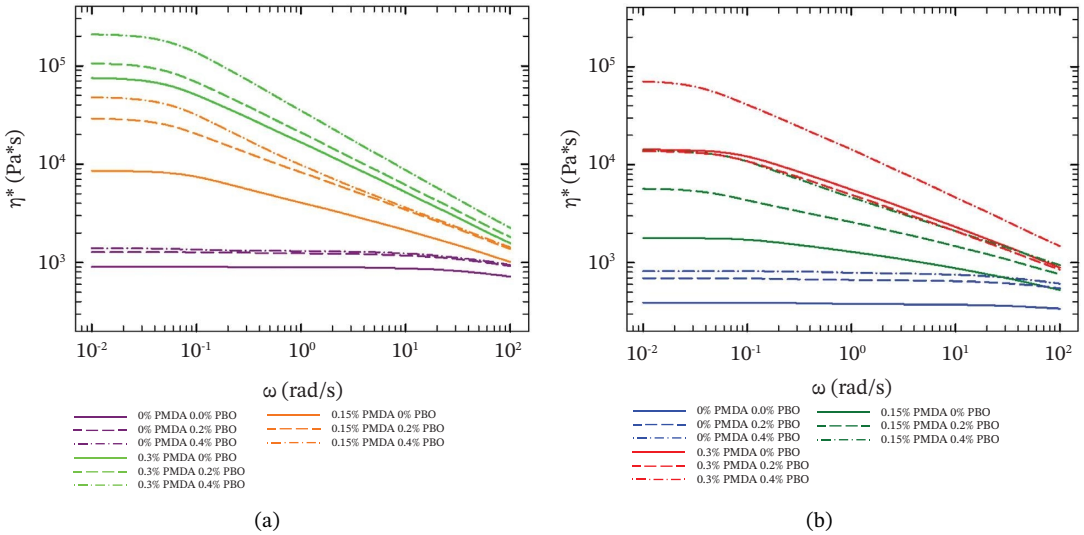

FIGURE 4 | Linear viscoelasticity of PET melts after the chain extension reaction. Data were obtained following the procedure outlined in Section 2.6. Complex viscosity (η^*) is plotted as a function of angular frequency (ω) for different concentrations of PMDA and PBO. (a) Virgin PET samples: curves compare formulations with 0%–0.3% PMDA and 0%–0.4% PBO. (b) Recycled PET samples: curves show the same range of PMDA and PBO concentrations.

The most interesting responses can be obtained from the variability chart of relaxation times, evaluated as detailed in Section 2.6. Here, the relaxation times exhibited by samples containing PBO only are comparable to those observed in neat PET, with a value of approximately 10^{-2} seconds. Indeed, the relaxation dynamics observed are consistent with those typically seen in linear chain polymers [48]. When PMDA is added to the melt and the system branches, the relaxation times become longer. Here, the combined effect of the two additives on relaxation dynamics can be clearly seen. As star-shaped macromolecules start to form via the reaction of the terminal hydroxyl groups of PET with anhydrides, PBO enables the growth of increasingly larger structures by connecting the remaining end of the linear PET chain through the saturation of the terminal carboxyl group. This process may result in the formation of macromolecules that possess an organized, more stable three-dimensional molecular architecture. It is noteworthy that for rPET, as the concentration of both additives increases, τ also rises. In contrast, for vPET-based samples, once the concentration of 0.15% PMDA and 0.4% PBO is exceeded, the relaxation time reaches a saturation level of approximately 20 s. This behavior suggests that, above a certain additive concentration, the relaxation dynamics of vPET-based samples are no longer sensitive to further increases in PMDA and PBO content. This may reflect the attainment of a characteristic molecular architecture controlling stress relaxation, rather than a continuous increase in effective chain length. This behavior is consistent with previous observations on long-chain branched polymers, where increases in branching density strongly affect the zero-shear viscosity, while the longest relaxation time is controlled by a limiting relaxation mechanism rather than by molecular weight alone [50]. As previously stated, the level of carboxyl end-groups, which can be reacted with PBO to form more complex architectures, appears to be higher in rPET because of chain scission during the recycling process [51, 52].

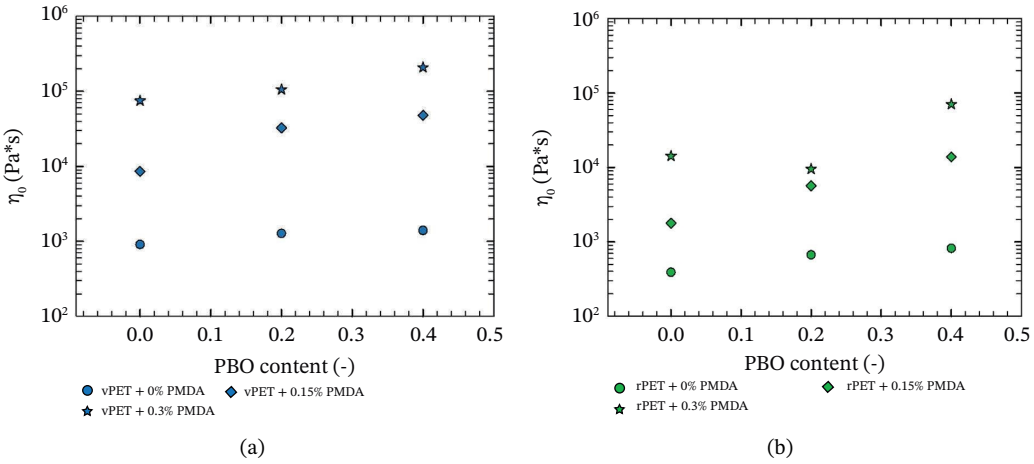

FIGURE 5 | Zero-frequency viscosities of polymer melts, (a) vPET samples and (b) rPET samples, as a function of PBO content. Curves are parametric in PMDA concentration. Data were extrapolated from the curves in Figure 4 after applying the procedure outlined in Section 2.6.

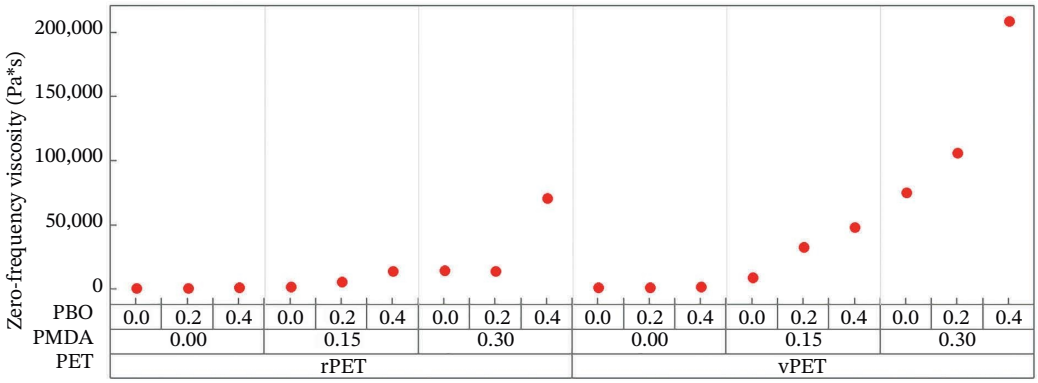

FIGURE 6 | Variability chart of zero-frequency viscosities of reacted samples.

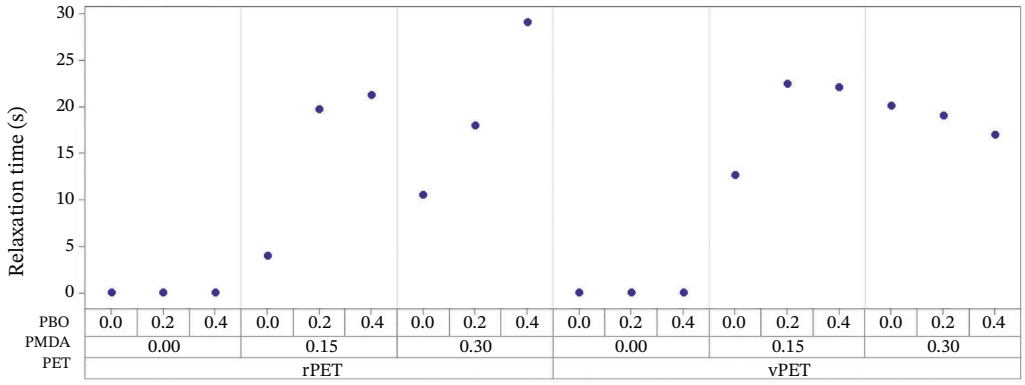

FIGURE 7 | Variability chart of relaxation times of reacted samples.

Larger macromolecules have slower global relaxation dynamics. The results obtained in this study demonstrate significant improvements in viscoelastic properties compared to single-additive systems reported in the literature. For vPET-based samples, the combination of PMDA and PBO at concentrations of 0.30% and 0.4%, respectively, resulted in an increase in zero-frequency/shear viscosity of approximately two orders of magnitude compared to neat vPET. This enhancement is substantially higher than that reported by Liu et al. [24] and Odet et al. [32], who observed increases of approximately one order of magnitude using PMDA alone at comparable concentrations, demonstrating the synergistic effect of combining bifunctional and tetrafunctional chain extenders. Regarding relaxation times, samples modified with both additives exhibited values of approximately 20 s for vPET, representing an increase of three orders of magnitude compared to neat PET ($\simeq 10^{-2}$ s). To the best of our knowledge, quantitative relaxation time data for chain-extended PET systems are not systematically reported in the literature, making this a novel contribution of the present work.

Figure 8(a)), showing the Pareto diagram of factors, facilitates the assessment of the effect of PET grades and additives on relaxation times. In general, variables whose bars in the diagram have longer lengths are considered more influential. In this instance, it is clear that the most significant contributions to melt relaxation times are from the PMDA and PBO concentrations, each

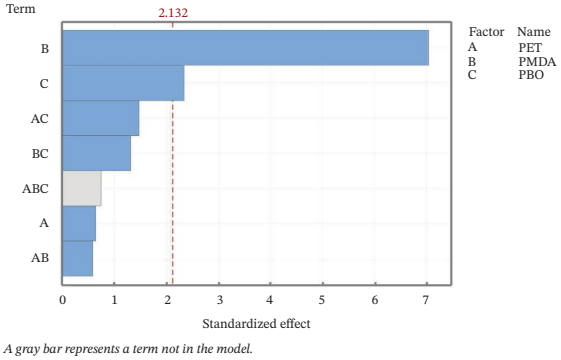

(a)

FIGURE 8 | (Continued)

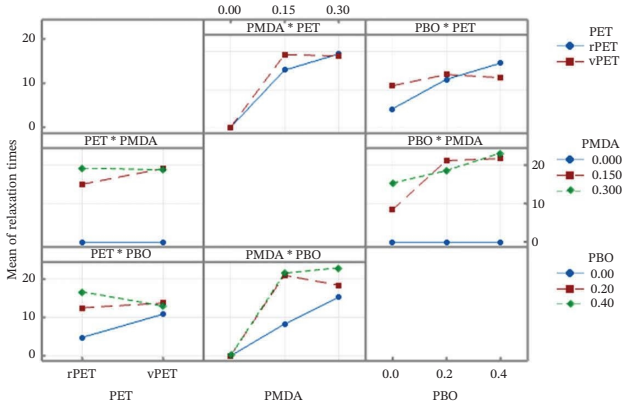

(b)

FIGURE 8 | (a) Pareto chart of standardized effects of the three variables on the relaxation times of samples. (b) Interaction plot of the three variables on the relaxation times of samples.

individually, and the combination of PET grade and PBO concentration. This supports the outcomes observed in the rheological tests and provides evidence of the efficacy of the experimental campaign. The interaction plot (Figure 8(b))) presents a visual representation of the impact of PET grade, PMDA, and PBO on the relaxation time. The y-axis displays the mean of relaxation time, while the *x*-axis represents the levels of variables and their combinations. The subplots indicate the relationship between two variables or the combined influence of three. The PET variable demonstrates a consistent pattern across all panels. The relaxation times for vPET are generally higher than those for rPET, indicating a significant effect of PET grade. Similarly, PMDA and PBO exhibit complex interaction patterns at various levels. Two-way interactions demonstrate that elevated PMDA levels are associated with increased relaxation times, particularly in the vPET case. In the PMDA-PBO panel, the relaxation times increase with the addition of both PMDA and PBO, indicating a combined effect of the two additives. The interaction between PBO and PET is evident, with rPET exhibiting higher relaxation times than vPET at the highest PBO concentration. The bottom-center panel illustrates the impact of PET, PMDA, and PBO on relaxation times. The highest relaxation times are observed at elevated PMDA and PBO levels.

4 | Conclusions

In this work, we investigated the effect of two additives, PMDA and PBO, on the rheological properties of both virgin and recycled linear PET. Real-time rheological monitoring of the reactions between PET and the chain extenders enabled us to identify the specific rheological responses of the different formulations at varying compositions and additive concentrations, closely mimicking conditions within an industrial reactive extruder. Furthermore, a global kinetic constant for the chain extension/branching reaction was derived. The linear viscoelasticity analysis of the reacted samples highlighted the distinct roles of the two additives: while PBO primarily acts as a chain extender for the linear PET chains, PMDA serves as a branching agent. Their combined action produces a system with a complex molecular architecture and enhanced rheological properties, which could be advantageous in industrial applications where tailored viscosity and relaxation dynamics are required, such as in foaming and blow molding processes. From an industrial perspective, these findings provide guidelines for the rational design of PET-based formulations with controlled processability and final properties. Nevertheless, the study is limited to laboratory-scale rheological measurements, and further validation under real extrusion and processing conditions will be necessary. Future work should also address the long-term stability of the modified systems, the influence of processing parameters such as shear and residence time, and the optimization of additive ratios to balance performance, cost, and sustainability.

Funding

No funding was received for this manuscript.

Conflicts of Interest

The authors declare no conflicts of interest.

Data Availability Statement

The data that support the findings of this study are available from the corresponding author upon reasonable request.

References

1. R. D. P. Daubeny, C. William Bunn, C. J. Brown, and W. Lawrence Bragg, "The Crystal Structure of Polyethylene Terephthalate," *Proceedings of the Royal Society of London-Series A: Mathematical and Physical Sciences* 226.1167, no. 1167 (1954): 531–542, https://doi.org/10.1098/rspa.1954.0273.

2. Independent Commodity Intelligence Services, *PET Market in Europe-State of Play (ICIS)* (Independent Commodity Intelligence Services, 2022).

3. W. C. Li, H. F. Tse, and L. Fok, "Plastic Waste in the Marine Environment: A Review of Sources, Occurrence and effects," *Science of the Total Environment* 566-567 (2016): 333–349, https://doi.org/10.1016/j.scitotenv.2016.05.084.

4. H. A. Leslie, M. J. M. van Velzen, S. H. Brandsma, A. Dick Vethaak, J. J. Garcia-Vallejo, and M. H. Lamoree, "Discovery and Quantification of Plastic Particle Pollution in Human Blood," *Environment International* 163 (2022): 107199, https://doi.org/10.1016/j.envint.2022.107199.

5. V. Dhaka, S. Singh, A. G. Anil, et al., "Occurrence, Toxicity and Remediation of Polyethylene Terephthalate Plastics. A Review,"

Environmental Chemistry Letters 20, no. 3 (2022): 1777–1800, https://doi.org/10.1007/s10311-021-01384-8.

6. I. Cusano, L. Campagnolo, M. Aurilia, S. Costanzo, and N. Grizzuti, "Rheology of Recycled PET," *Materials* 16 (2023): 9, https://doi.org/10.3390/ma16093358.

7. R. Kim, L. Delva, and K. Van Geem, "Mechanical and Chemical Recycling of Solid Plastic Waste," *Waste Management* 69 (2017): 24–58, https://doi.org/10.1016/j.wasman.2017.07.044.

8. C. Fiorillo, L. Trossaert, E. Bezeraj, et al., "Molecular and Material Property Variations During the Ideal Degradation and Mechanical Recycling of PET," *RSC Sustainability* 2, no. 12 (2024): 3596–3637, https://doi.org/10.1039/D4SU00485J.

9. F. Awaja and D. Pavel, "Recycling of PET," *European Polymer Journal* 41, no. 7 (2005): 1453–1477, https://doi.org/10.1016/j.eurpolymj.2005.02.005.

10. F. Perugini, M. L. Mastellone, and U. Arena, "Environmental Aspects of Mechanical Recycling of PE and PET: A Life Cycle Assessment Study," *Progress in Rubber, Plastics and Recycling Technology* 20.1, no. 1 (2004): 69–84, https://doi.org/10.1177/147776060402000106.

11. B. J. Holland and J. N. Hay, "The Thermal Degradation of PET and Analogous Polyesters Measured by Thermal Analysis–Fourier Transform Infrared Spectroscopy," *Polymer* 43.6, no. 6 (2002): 1835–1847, https://doi.org/10.1016/S0032-3861(01)00775-3.

12. G. Giannotta, R. Po', N. Cardi, et al., "Processing Effects on Poly(-Ethylene Terephthalate) From Bottle Scraps," *Polymer Engineering and Science* 34, no. 15 (1994): 1219–1223, https://doi.org/10.1002/PEN.760341508.

13. S. Saeid Hosseini, S. Taheri, Z. Ali, and A. Mehrabani-Zeinabad, "Hydrolytic Degradation of Poly(Ethylene Terephthalate)," *Journal of Applied Polymer Science* 103, no. 4 (2007): 2304–2309, https://doi.org/10.1002/app.24142.

14. M. Frounchi, "Studies on Degradation of PET in Mechanical Recycling," *Macromolecular Symposia* 144.1, no. 1 (1999): 465–469, https://doi.org/10.1002/masy.19991440142.

15. N. Torres, J. J. Robin, and B. Boutevin, "Study of Thermal and Mechanical Properties of Virgin and Recycled Poly(Ethylene Terephthalate) Before and After Injection Molding," *European Polymer Journal* 36, no. 10 (2000): 2075–2080, https://doi.org/10.1016/S0014-3057(99)00301-8.

16. R. Shamsi, G. M. M. Sadeghi, H. Vahabi, et al., "Hopes Beyond PET Recycling: Environmentally Clean and Engineeringly Applicable," *Journal of Polymers and the Environment* 27 (2019): 11, https://doi.org/10.1007/s10924-019-01507-x.

17. N. Bolanakis, E. Maravelakis, V. Papadakis, et al., "Valorization of Biochar as a Reinforcement Agent in Polyethylene Terephthalate Glycol for Additive Manufacturing: A Comprehensive Content Optimization Course," *Journal of Manufacturing and Materials Processing* 9 (2025): 2, https://doi.org/10.3390/jmmp9020068.

18. M. Petousis, N. Michailidis, V. Kulas, et al., "Valorization of Recycled Fine Powder Glass (RFPG) in Additive Manufacturing: Optimization of the RFPG Content in Polyethylene Terephthalate Glycol (PETG) and Multi-Response Analysis," *Cleaner Materials* 14 (2024): 100271, https://doi.org/10.1016/j.clema.2024.100271.

19. M. Petousis, N. Michailidis, V. Saltas, et al., "Mechanical and Electrical Proper-Ties of Polyethylene Terephthalate Glycol/Antimony Tin Oxide Nanocomposites in Material Extrusion 3D Printing," *Nanomaterials* 14 (2024): 9, https://doi.org/10.3390/nano14090761.

20. N. Michailidis, M. Petousis, V. Saltas, et al., "Investigation of the Effectiveness of Silicon Nitride as a Reinforcement Agent for-Polyethylene Terephthalate Glycol in Material Extrusion 3D Print-Ing," *Polymers* 16 (2024): 8, https://doi.org/10.3390/polym16081043.

21. S. Makkam and W. Harnnarongchai, "Rheological and Mechanical Properties of Recycled PET Modified by Reactive Extrusion," *Energy Procedia* 56 (2014): 547–553, https://doi.org/10.1016/j.egypro.2014.07.191.

22. K. S. J. Y. Jang, J. Seo, and J. Seo, "Chain-Extending Modification for Value-Added Recycled PET: A Review," *Polymer Reviews* 62, no. 4 (2022): 860–889, https://doi.org/10.1080/15583724.2022.2033765.

23. L. Incarnato, P. Scarfato, L. Di Maio, and D. Acierno, "Structure and Rheology of Recycled PET Modified by Reactive Extrusion," *Polymer* 41.18, no. 18 (2000): 6825–6831, https://doi.org/10.1016/S0032-3861(00)00032-X.

24. H. Liu, X. Wang, H. Zhou, W. Liu, and B. Liu, "The Preparation and Characterization of Branching Poly(Ethylene Terephthalate) and Its Foaming Behavior," *Cellular Polymers* 34, no. 2 (2015): 63–94, https://doi.org/10.1177/026248931503400202.

25. M. Härth and A. Dörnhöfer, "Film Blowing of Linear and Long-Chain Branched Poly(Ethylene Terephtha-Late)," *Polymers* 12 (2020): 7, https://doi.org/10.3390/polym12071605.

26. H. Arayesh, N. Golshan Ebrahimi, B. Khaledi, and M. K. Esfahani, "Introducing Four Different Branch Structures in PET by Reactive Processing––A Rheological Investigation," *Journal of Applied Polymer Science* 137, no. 41 (2020): 49243, https://doi.org/10.1002/app.49243.

27. R. Dhavalikar, M. Yamaguchi, and M. Xanthos, "Molecular and Structural Analysis of a Triepoxide-Modified Poly(Ethylene Terephthalate) From Rheological Data," *Journal of Polymer Science Part A: Polymer Chemistry* 41, no. 7 (2003): 958–969, https://doi.org/10.1002/pola.10641.

28. M. Xanthos, C. Wan, R. Dhavalikar, G. P. Karayannidis, and D. N. Bikiaris, "Identification of Rheological and Structural Characteristics of Foamable Poly(Ethylene Terephthalate) by Reactive Extrusion," *Polymer International* 53, no. 8 (2004): 1161–1168, https://doi.org/10.1002/pi.1526.

29. L. Xiao, H. Wang, Q. Qian, et al., "Molecular and Structural Analysis of Epoxide-Modified Recycled Poly(Ethylene Terephthalate) From Rheological Data," *Polymer Engineering & Science* 52.10, no. 10 (2012): 2127–2133, https://doi.org/10.1002/pen.23175.

30. J. Liu, Y. Lin, and X. Zhao, "Preparation of Long-Chain Branched Poly(Ethylene Terephthalate): Molecular Entanglement Structure and Toughening Mechanism," *Polymer Engineering & Science* 59, no. 6 (2019): 1190–1198, https://doi.org/10.1002/pen.25099.

31. V. Pandey, M. Seese, J. M. Maia, and D. A. Schiraldi, "Thermo-Rheological Analysis of Various Chain Extended Recycled Poly(Ethylene Terephthalate)," *Polymer Engineering & Science* 60, no. 10 (2020): 2511–2516, https://doi.org/10.1002/pen.25488.

32. F. Odet, N. Ylla, D. Karim, and P. Cassagnau, "Influence of Chain Extenders on Recycled Standard and Opaque PET Rheology and Melt-Spun Filament Properties," *ACS Applied Polymer Materials* 4, no. 11 (2022): 8290–8302, https://doi.org/10.1021/acsapm.2c01231.

33. C. W. Karl, B. Arstad, M. Shamsuyeva, et al., "Upgrading and Enhancement of Recycled Polyethylene Tereph-Thalate With Chain Extenders: In-Depth Material Characterization," *Industrial & Engineering Chemistry Research* 63.28, no. 28 (2024): 12277–12287, https://doi.org/10.1021/acs.iecr.4c00018.

34. P. K. George and E. A. Psalida, "Chain Extension of Recycled Poly(Ethylene Terephthalate) with 2,2′- (1,4-Phenylene) Bis(2-Oxazoline)," *Journal of Applied Polymer Science* 77, no. 10 (2000): 2206–2211, https://doi.org/10.1002/1097-4628.

35. S. John, "Additives for the Modification of Poly(Ethylene Terephthalate) to Produce Engineering-Grade Polymers," in *Modern Polyesters: Chemistry and Technology of Polyesters and Copolyesters* (John Wiley & Sons, Ltd, 2004), 495–540, https://doi.org/10.1002/0470090685.ch14.

36. E. L. Cano, J. M. Moguerza, and A. Redchuk, "Design of Experiments With R," in *Six Sigma With R: Statistical Engineering for Process Improvement* (Springer New York, 2012), 197–215, https://doi.org/10.1007/978-1-4614-3652-2_11.

37. S. Russo Spena, R. Pasquino, A. Sarrica, M. Delmonte, C. Yang, and N. Grizzuti, "Kinetics of Acid Hydrolysis of k-Carrageenan by in Situ Rheological Follow-Up," *Food Hydrocolloids* 144 (2023): 108953, https://doi.org/10.1016/j.foodhyd.2023.108953.

38. A. H. B. Victor, D. J. Read, and J. Ramírez, "Reptate Rheology Software: Toolkit for the Analysis of the Ories and Experiments," *Journal of Rheology* 64 (2020): 3, https://doi.org/10.1122/8.0000002.

39. N. Cardi, R. Po, G. Giannotta, E. Occhiello, F. Garbassi, and G. Messina, "Chain Extension of Recycled Poly(Ethylene Terephthalate) With 2, 2′—Bis(2—Oxazoline)," *Journal of Applied Polymer Science* 50, no. 9 (1993): 1501–1509, https://doi.org/10.1002/app.1993.070500903.

40. R. H. Colby, L. J. Fetters, and W. W. Graessley, "The Melt Viscosity-Molecular Weight Relationship for Linear Polymers," *Macromolecules* 20.9, no. 9 (1987): 2226–2237, https://doi.org/10.1021/ma00175a030.

41. F. Awaja, F. Daver, and E. Kosior, "Recycled Poly(Ethylene Terephthalate) Chain Extension by a Reactive Extrusion Process," *Polymer Engineering & Science* 44, no. 8 (2004): 1579–1587, https://doi.org/10.1002/pen.20155.

42. J. S. Forsythe, K. Cheah, D. R. Nisbet, et al., "Rhe-Ological Properties of High Melt Strength Poly(Ethylene Terephthalate) Formed by Reactive Extrusion," *Journal of Applied Polymer Science* 100, no. 5 (2006): 3646–3652, https://doi.org/10.1002/app.23166.

43. K. S. Seo and J. D. Cloyd, "Kinetics of Hydrolysis and Thermal Degradation of Polyester Melts," *Journal of Applied Polymer Science* 42, no. 3 (1991): 845–850, https://doi.org/10.1002/app.1991.070420330.

44. D. Kiryakova, K. George, and A. Atanassov, "Rheological Behaviour of Recycled and Virgin Polyethylenetere Thalate and Mixtures of Them," *Progress in Rubber, Plastics and Recycling Technology* 29 (November 2013): 255–270, https://doi.org/10.1177/147776061302900404.

45. Z. Yang, C. Xin, W. Mughal, X. Li, and Y. He, "High-Melt-Elasticity Poly(Ethylene Terephthalate) Produced by Reactive Extrusion With a Multi-Functional Epoxide for Foaming," *Journal of Applied Polymer Science* 135, no. 8 (2018): 45805, https://doi.org/10.1002/app.45805.

46. S. Trinkle, P. Walter, and C. Friedrich, "Van Gurp-Palmen Plot II–Classification of Long Chain Branched Polymers by Their Topology," *Rheologica Acta* 41, no. 1 (2002): 103–113, https://doi.org/10.1007/s003970200010.

47. M. Kruse and M. H. Wagner, "Rheological and Molecular Characterization of Long-Chain Branched Poly(Ethylene Terephthalate)," *Rheologica Acta* 56, no. 11 (2017): 887–904, https://doi.org/10.1007/s00397-017-1043-y.

48. M. Kruse, P. Wang, R. S. Shah, and M. H. Wagner, "Analysis of High Melt-Strength Poly(Ethylene Terephthalate) Produced by Reactive Processing by Shear and Elongational Rheology," *Polymer Engineering & Science* 59.2, no. 2 (2019): 396–410, https://doi.org/10.1002/pen.24936.

49. J. M. Dealy and K. F. Wissbrun, "Melt Rheology and Its Role in Plastics Processing: Theory and Applications," *Fluid Mechanics and Its Applications Series* (Springer, 1990).

50. J. Janzen and R. H. Colby, "Diagnosing Long-Chain Branching in Polyethylenes," *Journal of Molecular Structure* 486 (1999): 485–583, https://doi.org/10.1016/S0022-2860(99)00097-6.

51. P. Blais, M. Day, and D. M. Wiles, "Photochemical Degradation of Poly(Ethylene Terephthalate). IV. Surface Changes," *Journal of Applied Polymer Science* 17, no. 6 (1973): 1895–1907, https://doi.org/10.1002/app.1973.070170622.

52. D. N. Bikiaris and G. P. Karayannidis, "Effect of Carboxylic End Groups on Thermooxidative Stability of PET and PBT," *Polymer Degradation and Stability* 63, no. 2 (1999): 213–218, https://doi.org/10.1016/S0141-3910(98)00094-9.

Supporting Information

Additional supporting information can be found online in the Supporting Information section. *(Supporting Information)*

Supporting Information is available from the Wiley Online Library or from the author.